Available online at www.sciencedirect.com
ScienceDirect
Bioorganic & Medicinal Chemistry 15 (2007) 4651–4660
Bioorganic & Medicinal Chemistry

Zinc-(II) 2,9,16,23-tetrakis (methoxy) phthalocyanine: Potential photosensitizer for use in photodynamic therapy in vitro

Edith I. Yslas,[a] Edgardo N. Durantini[b] and Viviana A. Rivarola[a,*]

[a]*Departamento de Biología Molecular, Universidad Nacional de Río Cuarto, Agencia Postal Nro 3, X580BYA Río Cuarto, Argentina*
[b]*Departamento de Química, Universidad Nacional de Río Cuarto, Agencia Postal Nro 3, X580BYA Río Cuarto, Argentina*

Received 26 December 2006; revised 16 March 2007; accepted 26 March 2007
Available online 30 March 2007

Abstract—Photodynamic therapy (PDT) is an innovative treatment for several types of malignant and non-malignant disease. In the present study, $ZnPcOCH_3$ was investigated on a human larynx-carcinoma cell line (Hep-2) for its use in PDT. This drug exhibited favourable properties as a photosensitizer in vitro because $ZnPcOCH_3$ is able to penetrate efficiently in the cytoplasm of cultured cancer cells and is partially localized in lysosomes. The results show that $ZnPcOCH_3$-PDT-induced apoptosis by caspase dependent pathway. The new compound shows a good photosensitizing efficiency in vitro on Hep-2 cells, encouraging further in vivo studies.

1. Introduction

Photodynamic therapy (PDT) is a process in which the activation of photosensitizer (PS) by light results in the production of singlet oxygen and free radicals that are cytotoxics.[1] These highly reactive species can cause severe damage to the cellular constituents and are believed to be responsible for cell destruction.[2] PDT offers an alternative treatment to conventional therapies and is increasingly accepted as a therapeutic modality in oncology.[3,4]

Phthalocyanines are second generation PS which are receiving considerable attention in relation to their possible use in photodynamic treatment of several diseases.[5] These dyes show high molar extinction coefficients in the 680–700 nm region of the visible spectrum and generate singlet oxygen being the latter the main responsible for the cytotoxic effect in the cell inactivation. Phthalocyanines have favourable physical–chemical and spectral properties to be used as PS. Likewise, the photobiological properties of various phthalocyanine derivatives indicate that they can be promising photosensitizers for clinical application of PDT.[6]

PDT can induce cell death through necrosis or apoptosis both in vitro and in vivo.[7] Apoptosis is an active, controlled and energy-requiring process, whereas necrosis is a passive process, which is generally accompanied by a rapid loss of membrane integrity and metabolic homeostasis.[8] According to the biochemical and morphological features of apoptosis, there are several methods developed for its determination, such as microscopy, agarose gel electrophoresis and terminal deoxynucleotidyl transferase-(TdT)-mediated dUTPbiotin nick end labelling (TUNEL).[9]

Mitochondria are an important target in the cytotoxicity of PDT because this organelle is a critical site to release cytochrome *c* into the cytoplasm. Once in the cytosol, cytochrome *c* interacts with apoptosis-activating factor 1 (APAF 1) and activates the cascade of caspases. The latter triggers the final stage of apoptosis. Caspase-3 is the major caspase involved in induced apoptosis by many agents.

Cell death may occur either by apoptosis and/or necrosis depending on the cell line, the target for photosensitization, the intracellular concentration, the localization of the PS, the incubation protocols and the light doses.[10] The effect of the various factors in the photodynamic response remains yet to be elucidated.

In our previous work, it has been demonstrated that $ZnPcOCH_3$ produces singlet oxygen with a quantum

Keywords: Photodynamic therapy; Phthalocyanine; Cell death; Apoptosis.
* Corresponding author. Tel.: +54 0358 4676437; fax: +54 0358 4676232; e-mail: vrivarola@exa.unrc.edu.ar

0968-0896/$ - see front matter © 2007 Elsevier Ltd. All rights reserved.
doi:10.1016/j.bmc.2007.03.079

yield of 0.56 in tetrahydrofuran (THF). This is an appropriate value for phthalocyanine derivatives in this solvent. The fluorescence quantum yield of $ZnPcOCH_3$ presents a value of 0.26 ± 0.1. The fluorescence of this PS is appropriate for detection and quantification of the agent located in biological media.[11] The absorption and excitation spectra in different media indicate that this PS is essentially non-aggregated in these solutions.

In the present study, the properties of a novel zinc-(II) 2,9,16,23-tetrakis (methoxy) phthalocyanine ($ZnPcOCH_3$) for application in cancer therapy has been investigated, mainly by analyzing have cellular uptake, localization, alterations of lysosome and mitochondria, and death process induced in Hep-2 cells.

2. Results and discussion

2.1. Uptake of $ZnPcOCH_3$

In vitro determinations of intracellular drug accumulation indicate that, when incorporated into liposomes, $ZnPcOCH_3$ is taken up by Hep-2 cells rapidly and $ZnPcOCH_3$ shows a uptake that is initially very rapid at low incubation times (<3 h). Then it tends to a saturation value at incubation times $\geqslant 3$ h. These observations are similar to the result reported for HeLa treated with ZnPc[12] and NHIK 3025 cells.[13] The value of $ZnPcOCH_3$ uptake was estimated as 0.28 nmol/10^6 cells when the cultures were treated with 0.5 μM of PS. The response of this PS using 0.1 μM shows a similar profile to what we found at higher concentrations (0.5 μM), reaching a plateau value at ~0.05 nmol/10^6 cells. Based on this result it is possible to conclude that cellular uptake increased with PS concentration.[11]

2.2. Cytotoxic effect of $ZnPcOCH_3$

Figure 1 shows the survival of Hep-2 in the dark using $ZnPcOCH_3$ as the photosensitizer in different concentrations and incubation times. In the absence of light, 0.1 μM and 0.5 μM of $ZnPcOCH_3$ do not exhibit any decreasing viability. On the contrary, a concentration of 1 μM causes a significant decrease in cell survival.

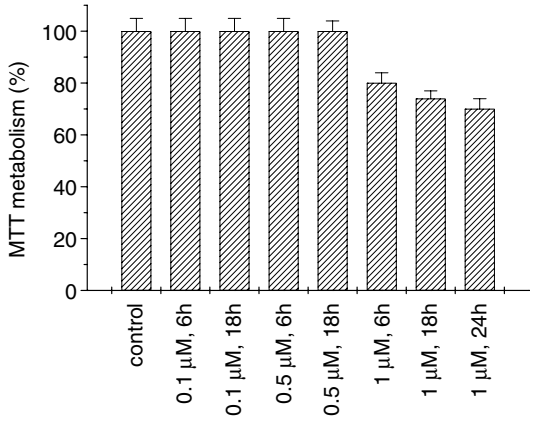

Figure 1. Effect of phthalocyanine concentration and incubation time on the MTT metabolism of Hep-2 cells in dark condition. Values are expressed as means ± standard deviation of three separate experiments, $p < 0.05$ control versus 0.1 and 0.5 μM of $ZnPcOCH_3$.

While 0.5 μM is non-toxic in the absence of light, it has a high photocytotoxicity which increases with the irradiation times. This photosensitizer, which is not toxic in the dark, induces a light dose-dependence loss of cell viability. The viability curve of Hep-2 cells incubated for 3 and 24 h in the dark and irradiated with increasing doses (Fig. 2) clearly shows a decrease of ~80% cell viability after an irradiation dose of 29 J/cm^2 24 h post-PDT. When the cultures were treated with 0.1 μM of PS, a decrease of 38% cell viability was observed (Fig. 2). The efficiency of cell photoinactivation is modestly influenced by the PS concentration despite the almost fivefold accumulation of $ZnPcOCH_3$ in the cell exposed to 0.1 μM compared with 0.5 μM concentration. The irradiation experiments show that the extent of cell photoinactivation steadily increases with irradiation time, as well as with phthalocyanine concentration.

2.3. Localization of $ZnPcOCH_3$ in lysosomes

The subcellular localization of PS is thought to play a critical role in determining the mode of cell death after PDT.[14] Fluorescence microscopy shows that Hep-2 cells, incubated at 37 °C for 3 h with 0.5 μM of $ZnPcOCH_3$, exhibit punctate fluorescence typical of ZnPc and mainly localized in a cytoplasmic region (Fig. 3).

Studies of cell image merge treated with the PS for 24 h and then with LysoTracker Green for 45 min show that $ZnPcOCH_3$ is located partially in the lysosomes. These images were processed using ImageJ 1.32j software. These data agree with previous work performed with other PSs.[15,16]

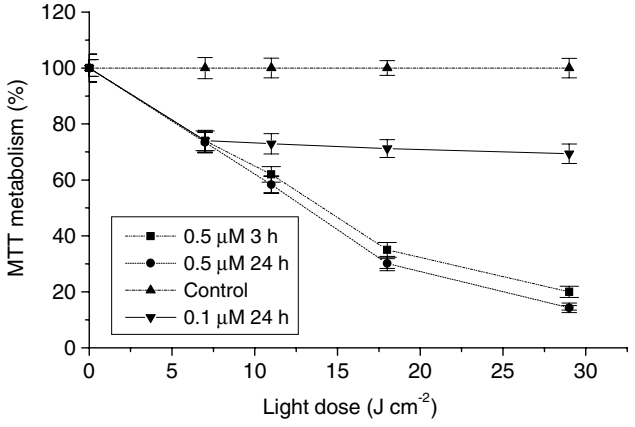

Figure 2. MTT metabolism of Hep-2 cells treated with phthalocyanine and exposed to visible light by different irradiation dose. (▲) cells irradiated with different irradiation dose; (■) $[ZnPcOCH_3] = 0.5$ μM, incubation time 3 h and 24 h post-PDT (●) $[ZnPcOCH_3] = 0.5$ μM, incubation time 24 h and 24 h post-PDT and (▼) 0.1 μM, incubation time 24 h and 24 h post-PDT. values are expressed as means ± standard deviation of three separate experiments, $p < 0.05$ light control versus 0.5 μM 3 h and 24 h and 0.1 μM 24 h.

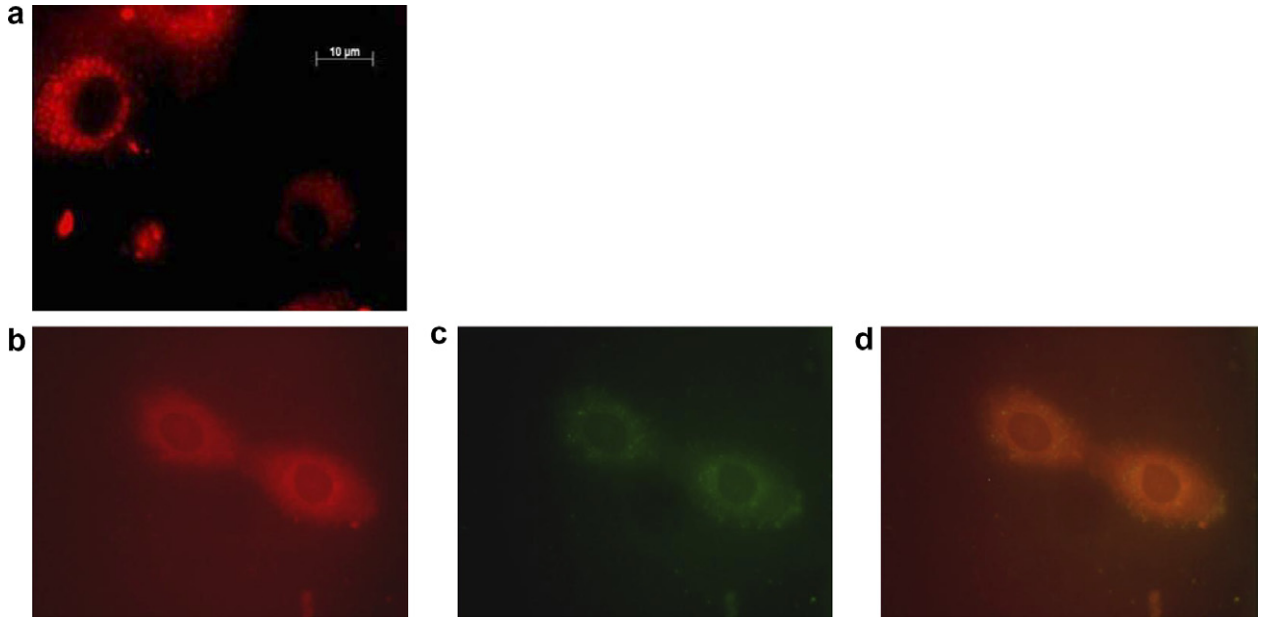

Figure 3. (a) Intracellular localization of $ZnPcOCH_3$ after 24 h of incubation with the sensitizer at 37 °C. $ZnPcOCH_3$-loaded Hep-2 cells were stained with LysoTracker Green DND-26. The red fluorescence of $ZnPcOCH_3$ showed an intracellular distribution 1000× (b) very similar to the fluorescence of the lysosomal probe LysoTracker Green (c) and co-localization was demonstrated by the yellow fluorescence of the overlay (d), 600×.

2.4. Photodynamic effect on cellular morphology

The percentage of cells undergoing apoptosis and necrosis after photodynamic treatment was determined microscopically by assessing morphology changes using Hoechst 33258, toluidine blue (TB), acridine orange (AO) and ethidium bromide (EB) staining.

The typical fluorescence pattern observed for untreated control Hep-2 cells after exposure to Hoechst 33258 dye is shown in Figure 4a. Minimal cytotoxicity is observed in dark control (Fig. 4b). The cell population observed for untreated and control dark samples (large nuclei and diffused chromatin) can be identified. When Hep-2 cells were irradiated with an 11 J/cm^2 light dose after 24-h incubation with 0.5 μM $ZnPcOCH_3$, the pattern shown in Figure 4c was obtained. Some cells presented typical apoptotic characteristics, such as condensed chromatin and fragmentation of the chromatin into apoptotic bodies. On the other hand, Figure 4d shows cells with necrotic characteristics, such as condensed nuclear chromatin and irregular nuclear fragmentation. Necrosis represents the prevailing mode of death for dark-incubated cells with $ZnPcOCH_3$ and irradiated with a 29 J/cm^2 light dose. The observation suggests that PDT treatment can induce both necrosis and apoptotic cell death depending on the light dose used. This result has been reported earlier.[17]

To demonstrate that this dose of PDT (11 J/cm^2) could cause apoptosis, we monitored changes in nuclear morphology. A minimum of 200 cells were counted for each treatment group. After 24 h $ZnPcOCH_3$-PDT, about 35% of cells began to display nuclear condensation and fragmentation, as indicated by Hoechst 33258 staining (Fig. 5). The remaining population corresponded to necrotic and ghost cells. The ghost cells are cells which have lost their nuclear membrane and have their DNA disintegrated.[18] Morphological changes were observed depending on the treatment conditions used when cells were stained with TB. Untreated Hep-2 cells showed their typical morphology with uncondensed chromatin, well-defined nucleoli and slight vacuolation of cytoplasm (Fig. 4e). After treatment with 0.5 μM of $ZnPcOCH_3$, cells seemed to be scarcely affected, presenting morphology quite similar to that of controls at any evaluated time (Fig. 4f). However, treatments with concentrations of 0.5 μM and 11 J/cm^2 dose of light (Fig. 4g) induced a variable amount of perinuclear vacuoles, cell rounding and shrinkage, and are accompanied with a progressive loss of cell–cell and cell–substrate adhesion. In addition, cells exposed to more dose of light (29 J/cm^2) showed the typical morphology of cell death by necrosis, characterized by nuclei with homogeneously condensed chromatin (pycnotic nuclei) and swelling, rupture and loss of membrane integrity (Fig. 4h).

The cells with a homogeneous chromatin pattern are AO negative (Figs. 4i and j), whereas those with condensed chromatin are AO positive. Condensation of chromatin in apoptotic bodies is a hallmark of apoptosis and it is observed in Figure 4k. While cells incubated in 0.5 μM $ZnPcOCH_3$, irradiated with 29 J/cm^2 and 24 h post-irradiation showed images of ethidium bromide-stained characteristic of necrotic cells (Fig. 4l).

Nuclear disintegration during apoptosis generates DNA strand breaks which can be identified by TUNEL assay. In order to confirm the characteristic morphological changes, a cytochemical assay for caspase-3 detection

was used. The cells treated with $ZnPcOCH_3$ in dark or light alone do not have any difference in green staining in comparison with untreated cells (Fig. 4m). Whereas the brown staining pattern shown in Figure 4n reveals apoptotic cells after PDT.

When $ZnPcOCH_3$ was present at a concentration of 0.5 μM with 11 J/cm^2, photoinactivation of the cells

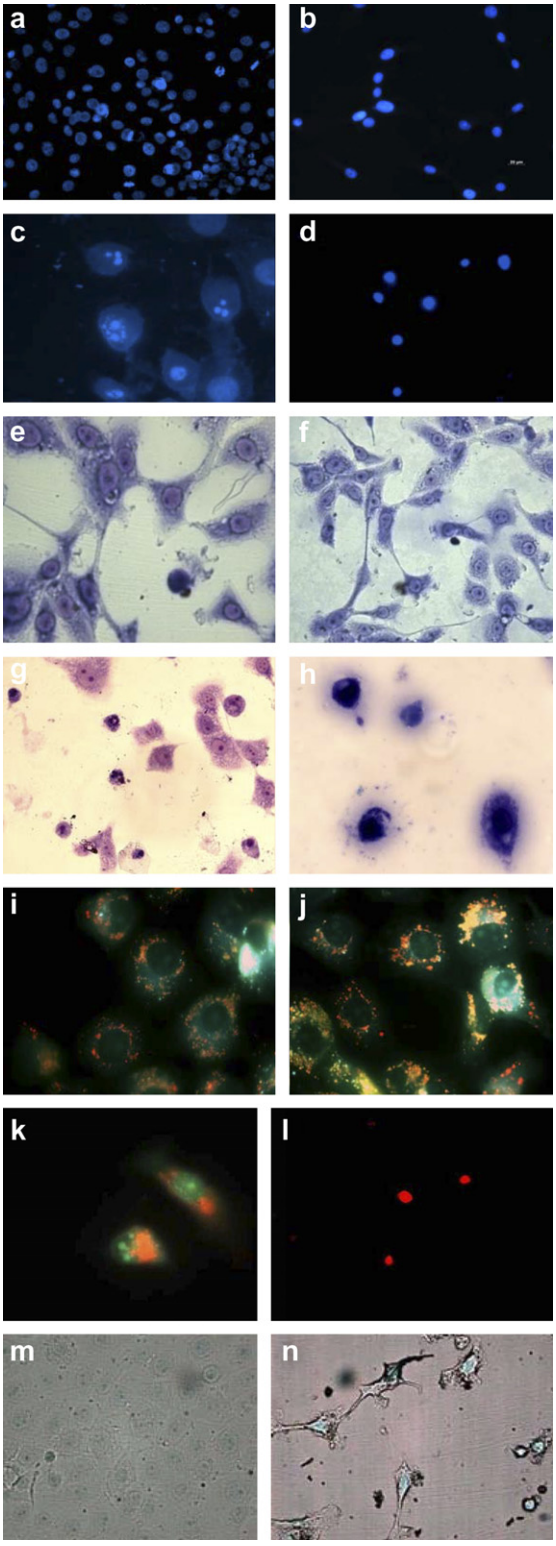

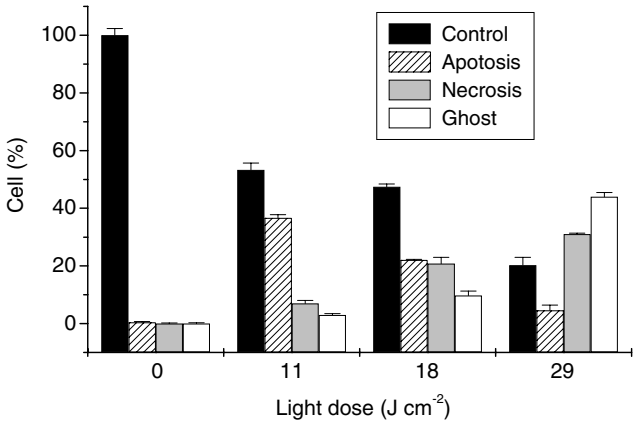

Figure 5. Evaluation of lethality mechanisms after incubation of Hep-2 cell with $ZnPcOCH_3$ (0.5 μM for 24 h) followed by different irradiation times. Control with non treated cells (1) and in the dark (2); cells irradiated with visible light for 11; 18; 29 J/cm^2. Values represent means ± standard deviation of three separate experiments.

24 h after-PDT causes apoptosis as the dominant mechanism of cell death. Under these conditions nuclear condensation and nucleosomal DNA fragmentation was observed as shown in Figure 6. These results suggest that the antiproliferative effects of $ZnPcOCH_3$ are associated with apoptosis and necrosis depending on the light dose in Hep-2 cells.

2.5. Expression and activity assay of caspase-3 in Hep-2 cells

The assay using the Hoechst 33258 staining and TUNEL assay show that Hep-2 cells incubated with $ZnPcOCH_3$ and irradiated trigger apoptosis. The occurrence of apoptotic process is confirmed by the presence of caspase-3 (which plays a crucial role and it is a key element in the execution phase of apoptosis) using an immunocytochemical method. Figure 7a shows untreated cells and (b) dark control cells stained for caspase-3. An immunoexpression is detected in the cytoplasm of brown staining pattern after 3 h of photodynamic treatment (Fig. 7c). This result clearly shows the induction of

Figure 4. Fluorescence images of Hoechst 33258-stained Hep-2 cells. (a) Untreated cells 200×; (b) Light dose = 0 (dark control), showing minimal dark cytotoxicity 400×; (c) cells incubated in 0.5 μM $ZnPcOCH_3$ for 24 h irradiated with 11 J/cm^2 when apoptotic nuclei became observable 1000× and (d) cells incubated in 0.5 μM $ZnPcOCH_3$ for 24 h irradiated with 29 J/cm^2. Images of Toluidine blue-stained Hep-2 cells. (e) Untreated cells; (f) light dose = 0 (dark control), showing minimal dark cytotoxicity; (g) 11 J/cm^2 when apoptotic nuclei became observable 400× and (h) with 29 J/cm^2. Images of Acridine Orange-stained Hep-2 cells. (i) Untreated cells 1000×; (j) light dose = 0 (dark control), showing minimal dark cytotoxicity 1000×; (k) 11 J/cm^2 when apoptotic nuclei became observable 1000×. Images of ethidium bromide-stained Hep-2 cells (l) cells incubated in 0.5 μM $ZnPcOCH_3$ for 24 h irradiated with 29 J/cm^2 29 J/cm^2 when necrotic nuclei became observable 600×. Images of TUNEL Hep-2 cells. (m) Untreated cells 630× and (n) Hep-2 cells incubated in 0.5 μM $ZnPcOCH_3$ for 24 h irradiated with 11 J/cm^2 and 24 h post-irradiation when apoptotic nuclei became observable 400×.

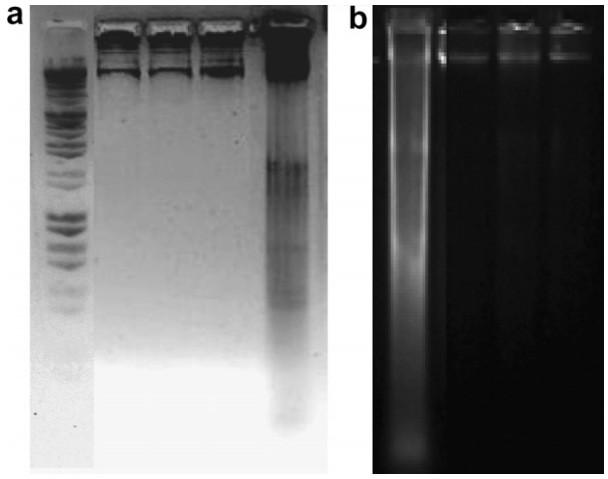

Figure 6. Detection of DNA fragmentation by 1.8% agarose gel electrophoresis in Hep-2 cells after inducing expression, small molecular weight DNA was prepared at various time points. (a) Lane 1 shows size markers, lane 2 control cancer cell, lane 3 light alone, lane 4 dark condition and lane 5 shows DNA isolated from Hep-2 cells following photodynamic treatment with [$ZnPcOCH_3$] = 0.5 μM, incubation time of 24 h irradiated with 11 J/cm^2 at 24 h post-PDT. Cells created a pattern characteristic of internucleosomal fragmentation and (b) lane 1 shows DNA isolated from Hep-2 cells following photodynamic treatment with [$ZnPcOCH_3$] = 0.5 μM, incubation time of 24 h irradiated with 29 J/cm^2 at 24 h post-PDT; lane 2 shows size markers, lane 3 control cancer cell and lane 4 light alone, lane 4 dark condition.

apoptosis through caspase-3 pathway in this cell line. To further confirm the observation that $ZnPcOCH_3$ and 11 J/cm^2 induce apoptosis, we tested caspase activity. These enzymes play a critical role in the execution of apoptosis and are responsible for many of the biochemical and morphological changes associated with the cell. Consequently caspase activity has been widely used to diagnose cells undergoing apoptosis.

Therefore, we monitored caspase-3-like activity at 24 h post-irradiation in cells treated with 0.5 μM for 24 h and irradiated at a light dose of 11 J/cm^2. The caspase-3-like activity is found to be higher in cells photodynamically treated when compared to dark controls and to untreated cells. As shown in Figure 7d, caspase-3 activity increased in PDT-treated cells, coinciding with results from the DNA fragmentation (Fig. 6) and TUNEL assay (Fig. 4).[19]

2.6. Lysosomal damage

Intracellular lysosomal rupture can be detected in intact cells by the fluorescence probe LysoTracker Green. This is selectively concentrated by intact lysosomes, resulting in green, granular fluorescence as observed in control cells (Fig. 8a). LysoTracker staining in non-treated and irradiated cells with 29 J/cm^2 is punctuate and occurs in perinuclear area. On the other hand, $ZnPcOCH_3$-sensitized Hep-2 cells show lysosomal damage and the loss of LysoTracker staining (Figs. 8c and d). In conclusion, $ZnPcOCH_3$-PDT produces lysosomal disruption that can be detected as a decrease in green fluorescence.

Treatment can induce cell membrane, mitochondrial, cytoskeletal and DNA damage, multiple independent

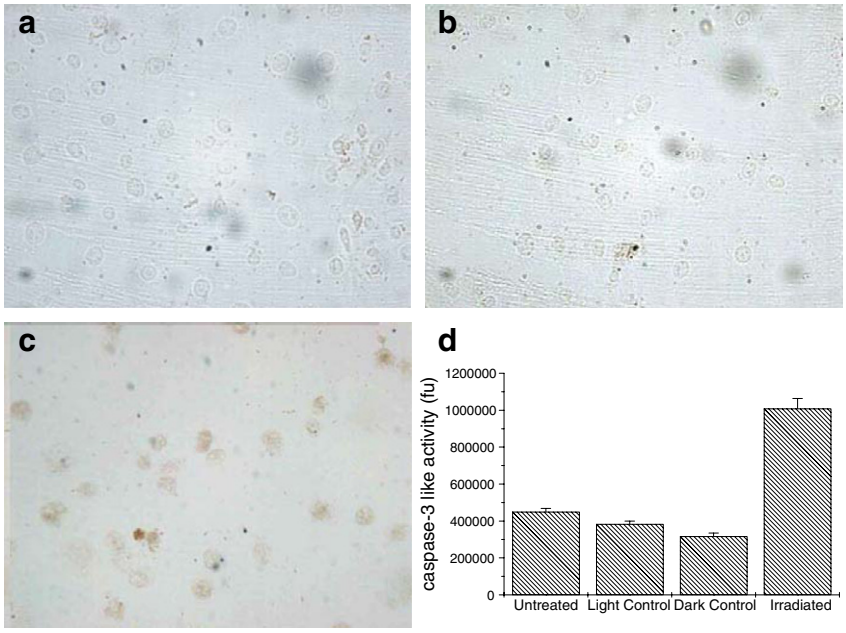

Figure 7. Inmunocytochemical staining of caspase-3 expression of Hep-2 cells following photodynamic treatment. (a) Untreated cells; (b) light dose = 0 (dark control); (c) cells treated with 0.5 μM $ZnPcOCH_3$ for 24 h and irradiated with 11 J/cm^2 and 3 h post-PDT 400× and (d) caspase-3 activity induced in cells after photodynamic treatment. Cells were incubated with 0.5 μM $ZnPcOCH_3$ in growth medium for 24 h in dark, subsequently irradiated with light (11 J/cm^2). Caspase-3 like activity was monitored after 24 h post-irradiation incubation. Each data point represents average ±SE from three experiments.

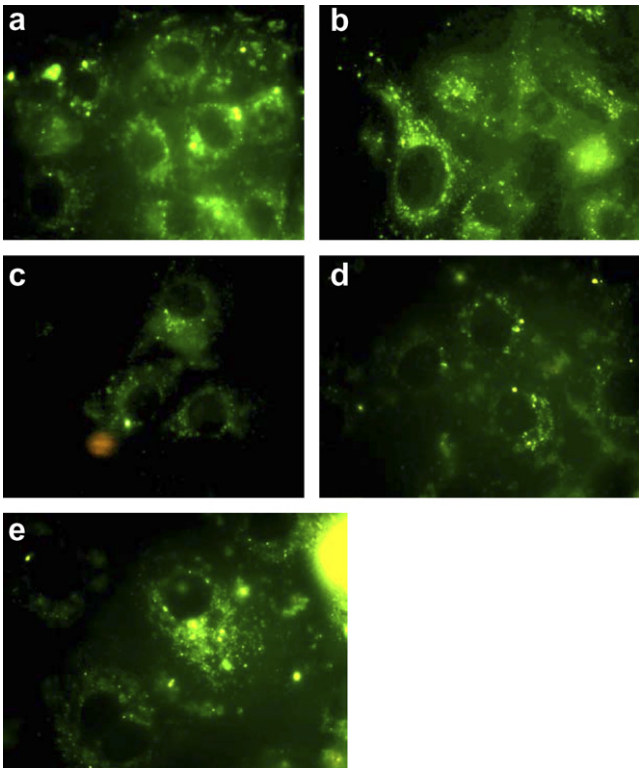

Figure 8. Fluorescence images of LysoTracker Green stained cells. (a) Light dose = 0 (dark control), (b) 29 J/cm^2 alone, (c) cells incubated with 0.5 μM $ZnPcOCH_3$ for 24 h and irradiated with 5 J/cm^2, (d) cells incubated with 0.5 μM $ZnPcOCH_3$ for 24 h and irradiated with 11 J/cm^2 and (e) cells incubated with 0.5 μM $ZnPcOCH_3$ for 24 h and irradiated with 29 J/cm^2, 1000×.

as well as dependent pathways could be involved in photodynamically induced apoptosis. Our study demonstrated that $ZnPcOCH_3$-PDT-induced caspase dependent pathway of apoptosis.

2.7. Studies on the change in the mitochondrial morphology

We investigated whether PDT-induced inner membrane permeabilization is associated with mitochondrial swelling. MitoTracker Red is taken up by polarized mitochondria. Once inside mitochondria, MitoTracker Red binds covalently to sulfhydryls and is retained by mitochondria after depolarization. Therefore, MitoTracker Red is a suitable dye to monitor mitochondrial volume changes under conditions that produce mitochondrial depolarization. Fifteen minutes after $ZnPcOCH_3$-PDT, mitochondrial morphology changes; mitochondria begin to round up and increase in diameter with 29 J/cm^2 (Fig. 9a, -PDT). In contrast, mitochondria do not depolarize in irradiated cells or in untreated cells and in the absence of light (Fig. 9a, PDT). Mitochondria initially appear filamentous, but gradually become swollen; and after 1 h of PDT most of them appear globular. The same results are obtained using Rh-123 fluorescence in control cells for light and PS, showing a heterogeneous and filamentous mitochondrial distribution (Fig. 9b, -PDT). After PDT the mitochondria present changes; initially they appear filamentous, but gradually become swollen and clear fragmentation of cytoplasm is observed with 5 J/cm^2 light dose after 30 and 60 min post-PDT (Fig. 9B, PDT). This swelling could lead to outer membrane rupture, causing the release of mitochondrial intermembrane proteins into the cytosol.

3. Conclusion

In the recent years, PDT has emerged as a promising therapeutic protocol to manage solid malignancies and non-malignant diseases. It is expected that higher intracellular concentrations of photosensitizer must provide

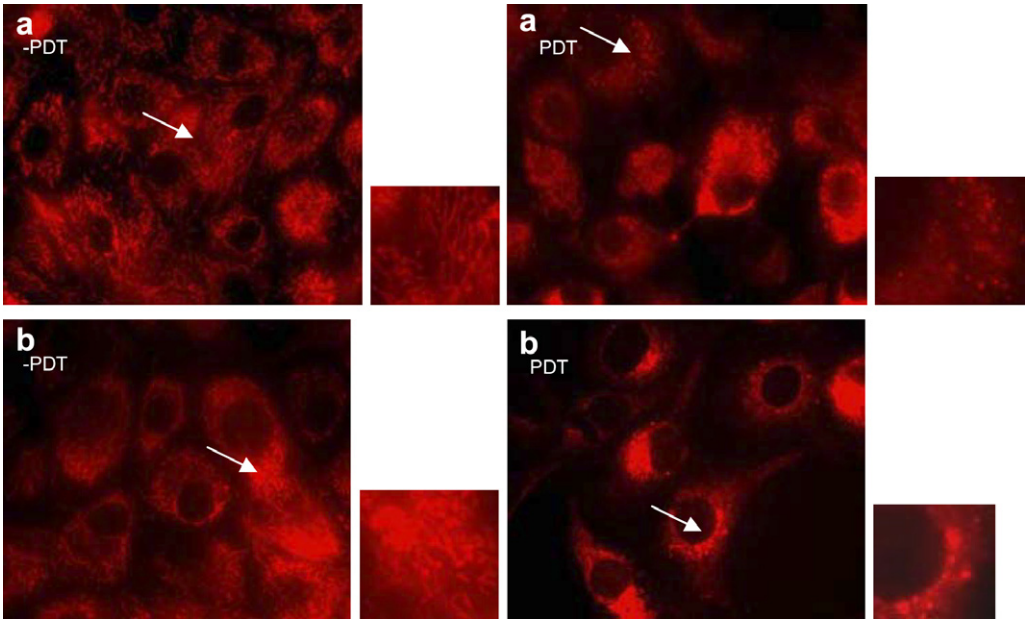

Figure 9. PDT induces mitochondrial swelling. (a) Cells were loaded with MitoTracker Red to monitor mitochondrial volume change, (-PDT) 29 J/cm^2 alone(PDT) 0.5 μM $ZnPcOCH_3$ + 29 J/cm^2 1000× and (b) cells were loaded with Rhodamine −123 to monitor changes in mitochondrial membrane potential (-PDT) 29 J/cm^2 alone and (PDT) 5 μM $ZnPcOCH_3$ + 5 J/cm^2 60 min post-PDT, 1000×.

higher photoinduced toxicity. In this paper, $ZnPcOCH_3$ is evaluated as a novel PS with potential application in PDT. Our results show that Hep-2 cells are sensitive to the phototoxic effects of $ZnPcOCH_3$ induced by light and this compound does not show cytotoxicity in dark condition.

Viability decreases proportionally according to the doses of visible light, reaching values of 80% of cell inactivation after a dose of 29 J/cm^2.

Apoptosis or necrosis can be encountered following a similar initial insult (radiation and cytotoxic drugs) and the balance between these cell death mechanisms depends upon the intensity of the injury. When the insult is applied at high intensity, immediate and irreversible damage which leads to cell necrosis is provoked. In this case, the rapid degradation of cell components is incompatible with the activation of biomolecules involved in the apoptotic pathway.

The present study indicates the involvement of caspases in PDT-induced apoptosis. Cell death by apoptosis or necrosis induced by PDT seems to be dependent on several parameters, such as drug concentration, incubation time, light dose, elapsed time after PDT and cell density.[20] In our study, different mechanisms of cell death are observed depending on the light doses. The apoptotic pathway occurs mainly at low light dose, while necrosis predominates at high light dose. Lam et al. have shown that PDT, using phthalocyanine 4, induces both apoptosis and necrosis depending on the light dose.[21] Furthermore, our results indicate that cells treated with $ZnPcOCH_3$ and irradiated by 11 J/cm^2 show caspase-3 activation, which leads to apoptotic cell death. Caspase activation determines $ZnPcOCH_3$-PDT-induced apoptosis in Hep-2 cells. In this work, the ability of Hep-2 cells to undergo apoptosis in response to PDT is demonstrated by Apo-Tag assay, nuclear morphology, DNA fragmentation, expression of caspase-3 and increase in caspase-3-like activity.

The photodynamic effect of $ZnPcOCH_3$ has been explained by cell destruction due to the production of reactive oxidative species such as singlet oxygen ($^1O_2$). Since $^1O_2$ can migrate a distance less than 0.02 μm after its formation, sites of photodamage will reflect the localization of sensitizer. For this reason, the localization of the photosensitizer determines the primary cellular target.

Fluorescence studies have shown that PS are localized in plasma membrane and organelles such as the mitochondria, lysosomes, Golgi complex, endoplasmic reticulum and nucleus.[22,23] Some authors postulated that hydrophobic PSs are incorporated into cells by endocytosis and therefore they should be first located in the lysosomal compartment. In any case, there are many hydrophobic or hydrophilic PSs for which a lysosomal localization has been described.[24] The phthalocyanine $ZnPcOCH_3$ used in this work is hydrophobic and preferentially accumulates in lysosomes.

Lysosomes are other organelles of photodamage. The photosensitizers' ability to damage lysosomes has been also reported by other molecules.[25,26] The immediate loss of membrane inner potential reflects a direct consequence of mitochondrial photodamage. After photodynamic treatment with $ZnPcOCH_3$ mitochondrial alteration is induced, showing disintegration of such filaments into smaller mitochondrial punctuate.

We hypothesize that PDT protocols employing lysosomal PS initiate apoptosis by lysosome disruption and liberation of proteases. This could be followed by a loss of mitochondrial transmembrane potential which stimulates the activation of caspase-3 and triggers apoptosis.

From the results shown in this work, it can be concluded that $ZnPcOCH_3$ is a promising PS agent. Its highly efficient ability to inactivate cultured tumour cells by apoptotic or necrotic modes depending on the light dose is an attractive photobiological feature. These results contribute to the knowledge of the PDT mechanism produced by $ZnPcOCH_3$ on Hep-2 carcinoma cell line. Therefore, $ZnPcOCH_3$ could constitute a useful tool for future research in PDT and tumour cell biology. At present, studies using BALB/c mice tumour models are being carried out in our laboratory.

4. Experimental

4.1. Cell line

The human larynx-carcinoma (Hep-2) cell line was maintained frozen in liquid nitrogen. The cells were cultured in monolayer at 37 °C in a humidified atmosphere with 5% CO_2 and grown in Dulbecco's modified Eagle's medium (DMEM) from Gibco (Gibco BRL; Paisley, UK) containing 7% heat-inactivated foetal bovine serum (FBS) and supplemented with 50 μg/mL gentamicin as antibiotic and 1% glutamine.

4.2. $ZnPcOCH_3$ uptake in Hep-2 cells

The incorporation of the PS into the phospholipid bilayer of the D,L-α-dipalmitoyl phosphatidylethanolamine was carried out according to the previously described procedure.[11] Cellular phthalocyanine uptake was determined by fluorescence spectroscopy (Spex Fluoro Max Fluorometer). Cells were first seeded (5.0×10^5) into 60-mm culture dishes in 4 mL of DMEM containing 7% foetal bovine serum and then incubated overnight at 37 °C. The cells were incubated in the dark at 37 °C for various time intervals (0–24 h) with 4 mL of DMEM containing 4% FBS and 0.5 μM $ZnPcOCH_3$. The cells were washed twice with PBS and harvested using a cell scraper. The cell number per mL was calculated by using a haemocytometer chamber (Improved Neubauer). Then the intracellular concentration was calculated considering the cell number after each incubation time. The uptake was determined by adding 1 mL of 6% aqueous sodium dodecyl sulfate (SDS) to 1 mL of cellular suspension after centrifugation; finally

1 mL of THF was added to the supernatant. The concentration of PS was calculated using a standard calibration curve of $ZnPcOCH_3$ in 2% of SDS in 2:1 water/THF, determined by fluorescence spectroscopy. The excitation and emission were set at 672 nm and 682 nm, respectively.

4.3. Cytotoxicity assay in dark condition

Hep-2 cells (3.0×10^5) were plated in 4 mL DMEM containing 7% FBS and incubated overnight at 37 °C in a humidified atmosphere with 5% CO_2. The medium was then removed and the cells were incubated for 6, 18 and 24 h with different concentrations of $ZnPcOCH_3$ (0.1–1 μM) in DMEM. Every experiment was compared to a control culture without PS. Cell survival was assessed by MTT assay (Sigma) based on the cellular conversion of a tetrazolium salt into a formazan in the presence of 3-(4,5-dimethyl-2-thiazolyl)-2,5-diphenyl-2*H*-tetrazolium bromide and Trypan blue exclusion test. The MTT assay was carried out as described by Carmichal et al.[27]

4.4. Photocytotoxicity assay

A Kodak slide projector with a 150 W bulb and equipped with a red filter was used for cell irradiation. The light was filtered through a 3-cm glass cuvette filled with water to absorb heat. The light fluence was measured with a radiometer (Laser Mate-Q, Coherent).

In this study, the Hep-2 cells were maintained at DMEM 7% FBS in a humidified atmosphere of 5% CO_2 at 37 °C. Then cells in exponential growth (3.0×10^5 cells per dish) were treated with 0.5 μM of $ZnPcOCH_3$ for 3 and 24 h or 0.1 μM of $ZnPcOCH_3$ for 24 h. The medium was then removed and the cells were washed with DMEM with 4% FBS. Then 4 mL of DMEM with 7% FBS was added and exposed to different light doses (5, 11 and 29 J/cm^2 and λ_{max} of 670 ± 5 nm). After light exposure, cultures were kept in the dark at 37 °C until assay. Additionally, identical plates for dark control and other controls without PS were prepared. Cell survival was assessed by measurement of MTT reduction at 24 h after irradiation.

4.5. $ZnPcOCH_3$ localization

Cells grown on microscopic glass coverslips were placed into 35-mm dishes and incubated with $ZnPcOCH_3$ (0.5 μM) for 3 h. Afterwards, cells were washed three times with PBS and observed under the fluorescence microscope using the appropriate excitation filters.

4.6. Lysosome and mitochondrial morphology

The alterations of lysosome functions following cell photosensitization with $ZnPcOCH_3$ were investigated by analyzing the decrease of intracellular fluorescence of LysoTracker Green DND-26 (Molecular Probes) at various post-irradiation times. Treated and untreated cell monolayers were incubated at 37 °C with LysoTracker Green (200 nM) for 45 min, washed with PBS and the fluorescence intensity of the probe in the cells was analyzed. The possible intracellular redistribution of $ZnPcOCH_3$ after irradiation was also investigated. The distribution of $ZnPcOCH_3$ fluorescence in Hep-2 cells was analyzed immediately and after 1- and 2-h irradiation. The intracellular localization of $ZnPcOCH_3$ was determined after 24- and 3-h incubation at 37 °C and was also compared to that of the mitochondrial probe MitoTracker Red. To monitor mitochondrial swelling, $ZnPcOCH_3$-treated cells' Mitochondria were stained with MitoTraker-Red FM (200 nM, 45 min, 37 °C) in DMEM containing 4% FBS and subsequently exposed to PDT. The activity of mitochondria was also determined with rhodamine 123 (Rh-123) after PDT. Rh-123 was used to investigate alterations in mitochondria because this dye is a potential sensitive cationic dye which crosses cell and mitochondria membrane within seconds and accumulates in negatively charged electrochemically functional mitochondria.[28]

Cells stained with LysoTracker Green DND-26, MitoTracker Red and Rh-123 were examined under a fluorescence microscope (Axiophot, Zeiss, Germany) using a colour camera (Axiocam, Zeiss, Germany) and Axiovision 4.3 software as well. BP 450-490, FT 510, for the fluorescence probes and BP 546 filters were used.

4.7. Cellular and nuclear morphology

Cells treated with $ZnPcOCH_3$ (0.5 μM) alone or subjected to light were collected and washed with PBS followed by fixation with cold methanol (−20 °C) for 10 min. The cells were stained either with 10 μg/mL Hoechst 33258, 0.5 mg/mL toluidine blue (TB) or 10 μg/mL acridine orange (AO) (Sigma) for 1 min, 45 s and 1 min, respectively. Stained cells were then washed and mounted on slides using DePeX.

Nuclear morphology of the cells was visualized with an Olympus fluorescence microscope using 330–380 nm excitations and measuring fluorescence at 420–450 nm. Three different fields of 200 cells per group treatment were scored, and the percentage of cells exhibiting apoptotic and necrotic morphology was determined with Hoechst.

4.8. DNA fragmentation and TUNEL

DNA fragmentation was analyzed by electrophoresis on agarose gel and by using the cytofluorimetric TdT-mediated dUTP-X nick end labelling (TUNEL) technique. Cells exhibiting apoptotic features were readily recognizable by intense, granular nuclear staining.

The TUNEL technique was applied on 10^6 cells by use of the in situ cell death detection kit (Boehringer Mannheim), following the manufacturer's instructions.

DNA samples were prepared for agarose gel electrophoresis following the procedure of Hopcia et al.[28] For DNA ladder assays, 10^6 cells were collected by centrifugation after PDT and washed with PBS. Cell pellets were resuspended in lysis buffer (100 mM NaCl,

10 mM Tris–HCl, 100 mM EDTA and 0.5% SDS) containing 0.1 mg/mL proteinase K and then incubated at 55 °C overnight. DNA was cleared from the lysates by centrifugation, extracted by using an equal volume of phenol/chloroform and then precipitated by adding absolute ethanol and 0.3 M ammonium acetate at −20 °C overnight. DNA was resuspended in sterilized water, treated with RNAse at 37 °C for 1 h and then analyzed by gel electrophoresis on 1.8% agarose gel stained with ethidium bromide (0.5 μg/mL).[29]

4.9. Immunocytochemical studies of caspase-3 and caspase assay in Hep-2 cells

The biotin–avidin–peroxidase (ABC) method was used for immunocytochemical studies.[30] Hep-2 cells were grown on a sterilized glass plate placed on a 35-mm diameter disc. The number of cells per dish was 3.0×10^5 in 2 mL of DMEM growth medium containing 7% FBS. After 24 h the medium was removed, the cells were incubated for 3 h with 0.5 μM of $ZnPcOCH_3$ in DMEM (2 mL) in the dark and then irradiated with a fluence rate of 29 J/cm^2. Cells were fixed for 10 min with cold acetone.

Following rehydration, cells were washed with PBS. Endogenous peroxidase was inhibited with hydrogen peroxide in distilled water (DW) for 30 min at 37 °C. Cells were then washed with PBS and incubated with normal horse serum for 30 min at room temperature (RT) in a wet chamber. After that, monoclonal mouse anti-caspase-3 antibody (Santa Cruz Biotechnology, Santa Cruz, CA) was added and incubated overnight at 4 °C in a wet chamber. After washing with PBS, cells were incubated for 1 h at RT in a wet chamber with the secondary-biotinylated antibody. Cells were washed again with PBS and incubated with ABC complex for 1 h at RT, washed and then developed with 3,3′ diaminobencidine (DAB, 6 mg in 10 mL PBS, adding 2 drops of 3% hydrogen peroxide in DW just before developing) for 3 min.

Two washings were done with DW; dehydration with ethanol (70%, 96% and 100%, 10–15 min each) and a pass through xylene (15 min). The coverslip was mounted with DePeX. The specificity of the immunohistochemistry was verified by omitting the primary antibody as a negative control. Cells were examined by Olympus microscopy.

On the other hand, the activity of caspase-3-like proteases from irradiated and unirradiated samples was determined following the protocol supplied by manufacturers (CPP32/caspase fluorometric protease assay, CHEMICAN International, Inc.). Twenty-four hours after irradiation, cells were released from the monolayer. Protein concentration was determined from a calibration curve using standard protein bovine serum albumin of known concentrations.

4.10. Statistical analysis

The results in figures and tables are from representative experiments ($n = 3$ independent experiments) which were run in triplicate. The data are expressed as means ± SD and the statistical analysis was performed by analysis of variance (ANOVA). Differences were considered significant when $p < 0.05$.

Acknowledgments

Authors are grateful to Consejo Nacional de Investigaciones Científicas y Técnicas (CONICET) of Argentina and Fundación Antorchas for financial support. E.N.D. and V.A.R. are Scientific Members of CONICET. E.I.Y. holds fellowship of CONICET.

References and notes

1. Weishaupt, K. R.; Gomer, C. J.; Dougherty, T. J. *Cancer Res.* **1976**, *36*, 2326–2329.
2. Girotti, A. Kessel, Ed.; *Photodynamic Therapy of Neoplastic Disease*, CRC Press: Boca Raton, 1990; Vol. 1, pp. 229.
3. Dougherty, T. J.; Gomer, C. J.; Henderson, B. W.; Jori, G.; Kessel, D.; Korbelik, M.; Moan, J.; Peng, Q. *J. Natl. Cancer Inst.* **1998**, *90*, 889–905.
4. Brown, S. B.; Brown, E. A.; Walker, I. *Lancet Oncol.* **2004**, *5*, 497–508.
5. Allen, C. M.; Scharman, W. M.; Van Lier, J. E. *J. Porphyr. Phthalocya* **2001**, *5*, 161–169.
6. Chan, W.-S.; Zuk, M.; Ben-Hur, E. Moser J G, Ed.; *Photodynamic Tumor Therapy, 2nd and 3rd Generation Photosensitizers;* Harwood Academic: Amsterdam, 1998; Chapter 2.4, pp. 63–73.
7. Plaetzer, K.; Kiesslich, T.; Verwanger, T.; Krammer, B. *Med Laser Appl.* **2003**, *18*(1), 7–19.
8. Mundle, S.; Iftikhar, A.; Shetty, V.; Dameron, S.; Wright-Quinones, V.; Marcus, B.; Loew, J.; Gregory, S.; Raza, A. *J. Histochem. Cytochem.* **1994**, *42*, 1533–1537.
9. Almeida, R. D.; Manadas, B. J.; Carvalho, A. P.; Duarte, C. B. *Bioch. et Bioph. Acta* **2004**, *1704*, 59–86.
10. Villanueva, A.; Vidania, R.; Stockert, J. C.; Canete, T. M.; Juarranz, A. *Handb. Photochem. Photobiol* **2003**, *4*, 79–117.
11. Yslas, E. I.; Rivarola, V.; Durantini, E. N. *Bioorg. Med. Chem.* **2005**, *13*(1), 39–46.
12. Villanueva, A.; Domínguez, V.; Polo, S.; Vendrell, V.; Sanz, C.; Cañete, M.; Juarranz, A.; Stockert, J. C. *Oncol. Res.* **1999**, *11*(10), 447–453.
13. Rodal, G. H.; Rodal, S. K.; Moan, J.; Berg, K. *J. Photochem. Photobiol.* **1998**, *45*, 150–159.
14. Chen, J. Y.; Cheung, N. H.; Fung, M. C.; Wen, J. M.; Leung, W. N.; Mak, N. K. *Photochem. Photobiol.* **2000**, *72*, 114–120.
15. Chernyaeva, E. B.; Greve, J. B. G.; Van Leeuwen, A. M. *Proc. SPIE* **1994**, *2083*, 62–70.
16. Leung, W. N.; Mak, N. K.; Yow, M. N. *Photochem. Photobiol.* **2002**, *75*, 406–411.
17. Fabris, C.; Valduga, G.; Miotto, G.; Borsetto, L.; Jori, G.; Garbisa, S.; Reddi, E. *Cancer Res.* **2001**, *61*, 7495–7500.
18. Villanueva, A.; Durantini, E.; Stockert, J. C.; Rello, S.; Vidania, R.; Cañete, M.; Juarranz, A.; Arranz, R.; Rivarola, V. *Anti Cancer Drug Des.* **2001**, *16*(6), 279–290.
19. Gorczyca, W.; Gong, J.; Darzynkiewicz, Z. *Cancer Res.* **1993**, *53*, 1945–1951.
20. Gupta, S.; Dwarakanath, B. S.; Muralidhar, K.; Jain, V. *J. Photochem. Photobiol. B.* **2003**, *69*, 107–120.

21. Lam, M.; Oleinick, N. L.; Nieminen, A. L. *J. Biol. Chem.* **2001**, *276*, 47379–47386.
22. Dummin, H.; Cernay, T.; Zimmermann, H. W. *J. Photochem. Photobiol. B.* **1997**, *37*(3), 219–229.
23. Woodburn, K. W.; Vardaxis, N. J.; Hill, J. S.; Kaye, A. H.; Philips, D. R. *Photochem. Photobiol.* **1991**, *54*, 125–732.
24. Ali, S. M.; Olivo, M. *Int. J. Oncol.* **2002**, *21*, 531–540.
25. Kessel, D.; Woodburn, K.; Henderson, B. W.; Chang, C. K. *Photochem. Photobiol.* **1995**, *62*, 875–881.
26. Gèze, M.; Morlière, P.; Mazière, J. C.; Smith, K. M.; Santus, R. *J. Photochem. Photobiol. B.* **1993**, *20*, 23–35.
27. Carmichal, J.; Degraff, W. G.; Gazdar, A. F.; Minna, J. D.; Mitchell, J. B. *Cancer Res.* **1987**, *47*, 936–942.
28. Johnson, L. V.; Walsh, M. L.; Chen, L. B. *proc. Natl. Acad. Sci.* **1980**, *77*(2), 990–994.
29. Gavrieli, Y.; Sherman, Y.; Ben-Sasson, S. A. *J. Cell Biol.* **1992**, *119*, 493–501.
30. Hsu, S. M.; Raine, L.; Fanger, H. *J. Histochem. Cytochem.* **1981**, *29*, 577–580.